LAWRENCE
LIVERMORE
NATIONAL
LABORATORY

LLNL-JRNL-426717

Local Properties of the Magnetic Field in a Snowflake Divertor

D.D. Ryutov, M. A. Makowski, M.V. Umansky

March 31, 2010

Plasma Physics and Controlled Fusion

Disclaimer

Local properties of the magnetic field in a snowflake divertor

D.D. Ryutov, M.A. Makowski, M.V. Umansky

Lawrence Livermore National Laboratory, Livermore, CA 94551, USA

Abstract

The power-law series for the poloidal magnetic flux function, up to the third-order terms, are presented for the case where two nulls of the poloidal magnetic field are separated by a small distance, as in a snowflake divertor. Distinct from the earlier results, no assumptions about the field symmetry are made. Conditions for the realization of an exact snowflake are expressed in terms of the coefficients of the power series. It is shown that, by a proper choice of the coordinate frame in the poloidal plane, one can obtain efficient similarity solutions for the separatrices and flux surfaces in the divertor region: the whole variety of flux surface shapes can be characterized by a single dimensionless parameter. Transition from a snowflake-minus to snowflake-plus configuration in the case of no particular symmetry is described. The effect of the finite toroidal current density in the divertor region is assessed.

I. Introduction

High heat loads on the plasma-facing components of tokamak divertors impose serious constraints on achievable performance of future tokamak-based reactors [1, 2]. One way of mitigating these problems may be transition to a second-order null of the poloidal magnetic field instead of a traditional first-order null. In other words, not only the poloidal field (PF), but also its first spatial derivatives would become zero. As the separatrix for the second-order null acquires a characteristic hexagonal form (Fig 1a), this configuration was called "a snowflake divertor" [3].

Potential advantages of the snowflake configuration stem from the fact that the poloidal flux expansion near the null-point becomes significantly larger than in the standard X-point divertor, the connection length from the midplane of the scrape-off-layer to divertor plates increases, and the radiative losses from the low-field zone become larger. In addition, the snowflake configuration may provide improved control over edge-localized modes via increased magnetic shear just inside the separatrix. These and other favorable features of the snowflake configuration have been studied in Refs. [3-8]. The snowflake has already been created on the TCV tokamak at Lausanne [9] and on the NSTX spherical torus at Princeton (see first brief announcement in Ref. [10]).

Other ways of reducing divertor heat loads include radiative divertors exploiting puff-and-pump techniques [11], Super-X divertors based on the significant increase of the major radius of the strike point [12], and the use of lithium coatings on the plasma-facing components [13]. These approaches will not be considered in our paper which is focused on the snowflake configuration.

Creating a second-order null requires specific adjustment of the currents in poloidal field (PF) coils. If the currents in PF coils are somewhat different from the "ideal" distribution, the exact snowflake configuration is replaced by a more complex

field structure. In Ref. 3, the resulting configurations were named "snowflake-plus" and "snowflake-minus", relating this transition to the magnitude of the current in PF coils (Fig.1 b,c). Both "plus" and "minus" configurations were identified in the aforementioned TCV experiment [9].

The poloidal field considered in Ref. 3, had a symmetry plane, as in Fig. 1. In this case, the snowflake-minus configuration was formed by two closely-spaced first-order nulls lying on the separatrix, whereas in the snowflake-plus configuration there remained one first-order null on the main separatrix. In Refs. [3, 5] it was shown that, if the deviation of the currents from the "ideal" distribution remained modest, the resulting configurations still maintained all the favorable properties of the exact snowflake.

In Ref. [7], it was shown that creating a snowflake (or near-snowflake) configuration in a particular tokamak, with given locations of PF coils, can be reached by merging (or near-merging) of two PF nulls by the proper adjustment of currents.

In this paper we generalize the analysis of Refs. [3, 5] to the geometries that do not possess any particular symmetry, as this more general situation is what is usually encountered in real tokamaks. Following an approach discussed in Refs. [3, 5], we use the power series expansions to represent the poloidal magnetic field in the area near the magnetic field null(s). The toroidicity effects are retained to the order consistent with the accuracy of the expansions. We produce general characterization of the magnetic field configuration, including the location of the nulls, orientation of the branches of the separatrix, and effects of the finite current density in the divertor region. The results can be used for a rapid assessment of possible PF structures in tokamaks, determining the location of the strike points, and evaluating poloidal flux expansion.

II. Basic equations and orderings

We consider toroidally-symmetric devices, where position of the point in the poloidal plane can be characterized by two components of cylindrical coordinates, r and z (Fig. 2). To analyze the field in the vicinity of the expected null (or two closely separated nulls), we introduce the coordinate x, which is small in the domain of interest. The major radius of the origin is R, and $r=R+x$. The coordinate z is also small in the divertor zone. The scale for the variation of the poloidal field on the global scale is the minor radius a, and we base our analysis on the inequalities $|x|,|z| << a < R$.

We introduce poloidal flux function $\Phi(x,z)$ so that

$$B_x = -\frac{1}{R+x}\frac{\partial \Phi}{\partial z};\quad B_z = \frac{1}{R+x}\frac{\partial \Phi}{\partial x}; \tag{1}$$

and $\nabla \cdot \boldsymbol{B} = 0$. With a standard assumption that the current density in the area of interest is negligibly small, this flux function has to satisfy Laplace equation

$$(R+x)\frac{\partial}{\partial x}\left(\frac{1}{R+x}\frac{\partial \Phi}{\partial x}\right) + \frac{\partial^2 \Phi}{\partial z^2} = 0 \tag{2}$$

Here we haven't used yet the assumption of the smallness of x and z.

As x and z are small compared to the minor radius, we now expand Φ in x and z up to the third order terms. The zeroth-order term can be dropped, as the field defined by Eqs. (1) is proportional to derivatives of Φ. Then, we have:

$$\Phi = l_1 x + l_2 z + q_1 x^2 + 2q_2 xz + q_3 z^2 + c_1 x^3 + c_2 x^2 z + c_3 x z^2 + c_4 z^3 + \ldots \quad (3)$$

We used symbols *l, q* and *c* for an easier identification of the corresponding terms as linear (*l*), quadratic (*q*), and cubic (*c*).

Before substituting these expressions to Eq. (2), we rewrite it as:

$$-\frac{\partial \Phi}{\partial x} + (R + x)\frac{\partial^2 \Phi}{\partial x^2} + (R + x)\frac{\partial^2 \Phi}{\partial z^2} = 0 \quad (4)$$

We have now to guarantee that the terms of the zeroth and the first order in *x,z* in the l.h.s. are zero (retaining higher order terms is possible, but they are small if we do not deviate too strongly from the vicinity of the origin; say, not further than 10-20% of the minor radius). Substituting Eq. (3) into (4) and setting the zeroth and the first order terms to zero, we find 3 conditions which are satisfied for any field:

$$-l_1 + 2q_1 R + 2q_3 R = 0; \quad (5)$$

$$2q_3 R + 6c_1 R^2 + 2c_3 R^2 = 0; \quad (6)$$

$$-2q_2 R + 2c_2 R^2 + 6c_4 R^2 = 0. \quad (7)$$

The presence of the parameter *R* is related to its presence in Eq. (1) for the magnetic field and does not mean that the terms not containing *R* are automatically smaller than others. In the general case, where one does not adjust currents in a particular way needed to create an exact snowflake, one has $l \sim qR \sim cR^2$.

The coefficients $c_{1\text{-}4}$ are determined by the global geometry of the plasma. As shown in Refs. [1-3], by the order of magnitude they are

$$c_{1-4} \sim RB_{pm}/a^2 \quad (8)$$

where B_{pm} is the poloidal magnetic field strength on the plasma boundary at the midplane, and *a* is the minor radius.

Expressions for the magnetic field, up to the 2nd order terms, are:

$$-(R + x)B_x = l_2 + 2q_2 x + 2q_3 z + c_2 x^2 + 2c_3 xz + 3c_4 z^2 \quad (9)$$

$$(R + x)B_z = l_1 + 2q_1 x + 2q_2 z + 3c_1 x^2 + 2c_2 xz + c_3 z^2 \quad (10)$$

To have a second-order null coinciding with the origin, one has to take

$$l_1 = 0, l_2 = 0 \quad (11)$$

(the condition that the magnetic field at the origin is zero), and

$$q_2 = 0, q_3 = 0 \quad (12)$$

(the condition that the first derivatives of the magnetic field are zero; note that, according to Eq. (5), the condition $q_1=0$ is then satisfied automatically). In other words, creating an exact snowflake configuration *at the desired point* requires imposing 4 constraints on the poloidal currents (the result presented in Refs. 3-5). Creating the first-order (standard) null would require imposing of only two constraints (11).

Consider now a case where conditions (11) and (12) are not exactly satisfied, but the terms *l* and *q* are small. If the latter is true, then we will have an approximate (or, in some cases, exact) snowflake in the vicinity of the origin. The magnetic configuration in this case is characterized by 9 parameters (two *l*'s, three *q*'s and four *c*'s). Equations (5)-(7) allow one to eliminate 3 parameters, leaving therefore 6 free parameters.

For l and q small, the action occurs in the zone of small x and z: $x,z\sim\varepsilon a$, where we have introduced a small parameter $\varepsilon<<1$. By inspecting Eq. (3), one sees that the ordering of the coefficients l and q is:

$$l \sim \varepsilon^2 a^2 c, \quad q \sim \varepsilon a c \tag{13}$$

The distance between the poloidal field null(s) and the origin is $\sim\varepsilon a$.

Out of 9 coefficients entering Eqs. (9), (10), we choose as "external" ones the following 6: l_1, l_2, q_2, q_3, c_1 and c_4. The other three parameters are then determined from Eqs. (5) – (7):

$$q_1 = -q_3 + \frac{l_1}{2R}; \quad c_3 = -3c_1 - \frac{q_3}{R}; \quad c_2 = -3c_4 + \frac{q_2}{R}. \tag{14}$$

The last terms in the r.h.s. of these expressions contain a small parameter $\varepsilon a/R$ compared to the first terms, and we will neglect them. So, we use the following expressions:

$$q_1 = -q_3; \quad c_3 = -3c_1; \quad c_2 = -3c_4. \tag{15}$$

Note that the toroidicity effects dropped out of our analysis; these effects appear only in the order $\varepsilon a/R$; their consistent account would require retaining the fourth-order terms in the expansion (4).

With these approximations made, we get from Eqs. (9), (10):

$$-(R+x)B_x = l_2 + 2q_2 x + 2q_3 z - 3c_4\left(x^2 - z^2\right) - 6c_1 xz \tag{16}$$

$$(R+x)B_z = l_1 - 2q_3 x + 2q_2 z + 3c_1(x^2 - z^2) - 6c_4 xz \tag{17}$$

III. Nulls, flux surfaces, and asymptotes

We start from identifying the position of PF nulls, i.e., from solving a set of equations $B_x=0$, $B_z=0$. Simple but lengthy calculations presented in Appendix, lead to the following result for the location of two field nulls:

$$x_{1,2} = \xi \pm \sqrt{\frac{P}{2} + \sqrt{\frac{P^2}{4} + Q^2}}\ ; \quad z_{1,2} = \zeta \pm (signQ)\sqrt{-\frac{P}{2} + \sqrt{\frac{P^2}{4} + Q^2}} \quad . \tag{18}$$

where

$$\xi = \frac{q_3 c_1 + q_2 c_4}{3\left(c_1^2 + c_4^2\right)}, \quad \zeta = \frac{q_2 c_1 - q_3 c_4}{3\left(c_1^2 + c_4^2\right)}, \tag{19}$$

and

$$P = \frac{l_2 c_4 - l_1 c_1}{3\left(c_1^2 + c_4^2\right)} + \xi^2 - \zeta^2, \quad Q = \frac{l_2 c_1 + l_1 c_4}{6\left(c_1^2 + c_4^2\right)} + \xi\zeta. \tag{20}$$

In the case where both P and Q are zero, the two roots (x_1, z_1) and (x_2, z_2) merge. According to a consideration presented in Ref. 7, this gives rise to an exact snowflake. Unless conditions (11), (12) are satisfied, this snowflake will not be situated in the origin, but rather in the point $x=\xi$, $z=\zeta$.

As mentioned in Ref. 3, the exact snowflake is topologically unstable. This means that even infinitesimal change of the system parameters leads to its splitting into configuration with two PF nulls (albeit separated by a small distance if perturbations are small). To contrast this to an ordinary first-order X-point, we note that, for a small change of parameters, the null just slightly moves, but the general shape of the separatrix does not change.

One special case of such a splitting of a snowflake configuration is the one where the two nulls end up lying on the same separatrix (like in Fig. 1 c). As, in a symmetric case, this configuration would correspond to smaller-than-optimum current in the divertor coils [3], it was called "a snowflake-minus." In some sense, this configuration is analogous to a double-null divertor [14], although the two nulls are now situated not in the upper and lower parts of the tokamak and separated by a distance of a meter or so, but close to each other, within less than ~10 cm. One can show (we skip this simple derivation) that the configuration with two nulls on the same separatrix is realized if

$$Q = \frac{\sqrt{3}}{2} P, \quad P < 0. \tag{21}$$

The snowflake-minus configuration is also topologically unstable in the sense that the infinitesimal change of the plasma parameter leads to a configuration where the nulls lie on two different separatrices.

The distance between the nulls is, in the most general case,

$$D = \sqrt{(x_1 - x_2)^2 + (z_1 - z_2)^2} = 4\sqrt{P^2 + 4Q^2} \tag{22}$$

Now we discuss the shape of the flux surfaces. We use a flux function that accounts for conditions (15):

$$\Phi = l_1 x + l_2 z - \\ -q_3 x^2 + 2q_2 xz + q_3 z^2 + \\ c_1 x^3 - 3c_4 x^2 z - 3c_1 x z^2 + c_4 z^3 \tag{23}$$

At large x and z, Eq. (23) determines the shape of the asymptotes for the separatrix. Equation characterizing the tangents to asymptotes in the x,z plane is:

$$c_1 - 3c_4 t - 3c_1 t^2 + c_4 t^3 = 0, \quad t \equiv z/x. \tag{24}$$

This asymptotes are a good representation os separatrices at the distances exceeding the distamnce between the nulls but still small compared ot the minor radius.

Equation (24) always has three real roots, corresponding to three asymptotes. One can show that these three asymptotes are separated by 120 degrees (i.e., when one considers both positive and negative x, there are 6 rays separated by 60 degrees). Conversely, by specifying the orientation of the ray, one can find the ratio c_1/c_4:

$$\frac{c_1}{c_4} = \frac{t\left(t^2 - 3\right)}{3t^2 - 1} \tag{25}$$

The parameter t is related to the angle α between a ray in the first quadrant and axis x:

$$t = \tan\alpha, \tag{26}$$

see Fig 3a. Due to the presence of 6 rays equidistant in α, the range of α can be chosen as $0 < \alpha \le \pi/3$.

Obviously, by rotating the (x, z) frame, one can always orient the axis z so that it would become a bisector for the asymptotes 1 and 2 (Fig. 3 b). This orientation corresponds to $\alpha = \pi/3$, so that c_1=0. We will also identify the confinement region as the region lying between two upward-pointing asymptotes (shaded region in Fig. 3b) and call the branches of the separatrix highlighted in red in Fig. 3b the "main separatrix."

Under condition c_1=0, expressions for ξ, ζ, P and Q are greatly simplified. We get:

$$\xi = \frac{q_2}{3c_4}, \quad \zeta = -\frac{q_3}{3c_4}, \tag{27}$$

$$P = \frac{l_2}{3c_4} + \frac{q_2^2 - q_3^3}{9c_4^2}, \; Q = \frac{l_1}{6c_4} - \frac{q_2 q_3}{9c_4^2}. \tag{28}$$

In what follows, we assume that $c_4>0$. This choice of the sign corresponds to the following convention regarding the magnetic flux Φ: it is positive well inside the plasma confinement region. The flux function, after the just described rotation of the frame, becomes

$$\begin{aligned} &\Phi = l_1 x + l_2 z - \\ &-q_3 x^2 + 2q_2 xz + q_3 z^2 + \\ &-3c_4 x^2 z + c_4 z^3 \end{aligned} \tag{29}$$

The rotation, obviously, leads to a re-definition of the coefficients in this expansion (i.e., the coefficients l and q in Eq. (29) are different from those in Eq. (23)), as well as re-definition of the coordinates x and z, but, for brevity, we retain the old notation.

Consider the situation discussed in Refs. [1, 3], where the system was assumed to have a symmetry plane x=0. This symmetry corresponds to the absence of the terms odd in x in Eq. (29), i.e. to l_1=0, q_2=0. Equation (28) shows that exact snowflake will then be produced if

$$l_2 = \frac{q_3^2}{3c_4} \tag{30}$$

and will be situated at $z = -\frac{q_3}{3c_4}$. The shape of several flux surfaces for q_3=0 is shown in Fig. 4a.

If condition (30) is violated, one can have two qualitatively-different cases. The case

$$l_2 < \frac{q_3^2}{3c_4} \tag{31}$$

corresponds to a “snowflake-plus” configuration, where only one first-order null remains on the main separatrix (Fig. 4 b), whereas the case

$$l_2 > \frac{q_3^2}{3c_4} \tag{32}$$

corresponds to a “snowflake-minus” configuration, with two nulls on the main separatrix (Fig. 4c).

On the other hand, if the system does not possess a symmetry plane, possible deviations from the exact snowflake lead to the formation of more complex configurations that we discuss in Sec. IV.

IV. Similarity properties

We have shown that, by a proper rotation of the coordinate frame, one can always orient the confinement region in such a way that the axis z will form equal angles with the separatrices limiting the confinement region, as shown in Fig. 3 b. [An orientation with the confinement region above the divertor is typical for most of tokamaks.] After

that, by moving the origin, one can always put it into that of two nulls that lies on the main separatrix. The fact that one of two nulls is situated in the origin, automatically means that $l_1=l_2=0$. [The translation of the coordinate system will, again, lead to the redefinition of coefficients q and coordinates x and z, but we, again, keep the notation unchanged.] After that, one can easily show that the expression for the coefficients q_2 and q_3 can be expressed in terms of the position of the second null (which we denote by upper-case X and Z), and the overall expression for the flux function (29) becomes:

$$\Phi = c_4\left(\frac{3Z}{2}x^2 + 3Xxz - \frac{3}{2}Zz^2 - 3x^2z + z^3\right) \tag{33}$$

We note that the coefficient c_4 is determined by the global structure of the magnetic field and is not affected by variation of the field in the divertor region, the variation described by the location of the second null. We therefore come to a conclusion, that most general shape of the snowflake flux-surfaces in the divertor region can be fully characterized by only two parameters, X and Z, having a simple geometrical sense (location of the second null). The poloidal magnetic field in this zone, aside from the normalizing factors, is also fully characterized by these two parameters:

$$B_x = -\frac{3c_4}{R}\left(Xx - Zz - x^2 + z^2\right) \tag{34}$$

$$B_z = \frac{3c_4}{R}\left(Zx + Xz - 2xz\right) \tag{35}$$

The main separatrix, the one that passes through the origin, corresponds to $\Phi=0$,

$$\frac{3Z}{2}x^2 + 3Xxz - \frac{3}{2}Zz^2 - 3x^2z + z^3 = 0 \tag{36}$$

The separatrix passing through the second null is determined by equation

$$\frac{3Z}{2}x^2 + 3Xxz - \frac{3}{2}Zz^2 - 3x^2z + z^3 = \frac{Z}{2}\left(3X^2 - Z^2\right) \tag{37}$$

The r.h.s. of this equation is determined by substituting $x=X$, $z=Z$ to the l.h.s. One can relate these two parameters to the general set of the coefficients entering expansion (23). An example of the separatrices and nearby flux surfaces for the cases X=1, Z=-0.2; X=*1*, $Z=-\sqrt{3}$; X=0.2, Z= -1 is presented in Figs. 5 *a-c*.

The flux surfaces adjacent to the separatrices can be characterized by the difference $\delta\Phi$ of the flux function on a given flux surface from its value exactly on the separatrix. The parameter $\delta\Phi$ characterizes the distance Δ between the flux surface and the separatrix in the tokamak midplane. According to Eq. (8), by the order of magnitude, $\delta\Phi \sim RB_{pm}\Delta$. Then, using Eq. (33), one finds that the equation for the flux surface adjacent to the main separatrix is

$$\frac{3Z}{2}x^2 + 3Xxz - \frac{3}{2}Zz^2 - 3x^2z + z^3 = -Ca^2\Delta \tag{38}$$

where C>0 is a dimensionless coefficient of order 1, and the sign is chosen in such a way that positive Δ corresponds to the area just outside the separatrix. The analogous equation should be used for the flux surfaces adjacent to the second separatrix, with Δ measured from this second separatrix in the midplane.

Instead of X and Z, one can alternatively characterize the magnetic field by two other parameters, the distance D between the nulls, and the angle ϑ formed by the

horizontal axis and the line connecting the nulls (Fig. 5b), and measured towards the lower half-space, so that

$$X = D\cos\vartheta, \quad Z = -D\sin\vartheta \tag{39}$$

As the null lying on the main separatrix does, due to our choice of the origin, coincide with the origin, we have to assume that $\vartheta > 0$ (i.e., the second null lies below the horizontal axis). The parameters D and ϑ can be expressed through the input parameters *l, q, c* in Eq. (3), but we do not present these lengthy expressions here.

Using Eqs. (36)-(37), and introducing dimensionless variables $\tilde{x} = x/D$, $\tilde{z} = z/D$, one finds equations characterizing the shape of the separatrices by just *one* parameter, ϑ (up to a scaling factor D):

$$-\frac{3\sin\vartheta}{2}\tilde{x}^2 + 3\tilde{x}\tilde{z}\cos\vartheta + \frac{3\sin\vartheta}{2}\tilde{z}^2 - 3\tilde{x}^2\tilde{z} + \tilde{z}^3 = 0 \tag{40}$$

$$-\frac{3\sin\vartheta}{2}\tilde{x}^2 + 3\tilde{x}\tilde{z}\cos\vartheta + \frac{3\sin\vartheta}{2}\tilde{z}^2 - 3\tilde{x}^2\tilde{z} + \tilde{z}^3 = -\frac{\sin 3\vartheta}{2} \tag{41}$$

This remarkable self-similarity is of course a consequence of the power-law representation of the flux function up to the terms of the 3rd order. The nearby flux surfaces can be obtained by adding to or subtracting from the r.h.s. of Eqs. (40), (41) some small number δ.

Our results show that the parameter ϑ controls transition between two very different divertor configurations. If one starts with ϑ=0, one obtains a "symmetric snowflake-minus", like the one shown in Fig. 4 c. When ϑ is in the range $0<\vartheta<\pi/3$, we have a configuration that can be called an "asymmetric snowflake-minus". It is characterized by the presence of two nearby separatrices. A significant plasma volume is formed near the bottom of the confining region (zone marked by the number 1 in Fig. 5a). The presence of this zone would increase the radiative losses from the plasma on its way from the outer SOL to the strike-point 2 in Fig. 5a. For the case where the distance between the separatrices is less than the midplane SOL thickness, significant part of the plasma would reach the strike point 3. This would help in reducing the heat flux on the divertor plates. The distance $\Delta_{1,2}$ between two separatrices in the midplane is controlled by the value of ϑ. According to Eqs. (38)-(41),

$$\Delta_{12} = \frac{D^3 \sin 3\vartheta}{2Ca^2} \tag{42}$$

For a given D, the maximum distance between the separatrices is reached at $\vartheta=\pi/6$. For $\vartheta>\pi/6$, the distance decreases, and, at $\vartheta=\pi/3$ becomes zero (Fig. 5b). This is just a rotated symmetric snowflake-minus configuration of Fig. 4c. For larger values of ϑ, we obtain a configuration which can be called an "asymmetric snowflake-plus" (Fig. 5c). Here, the confinement region is surrounded by a single separatrix. For ϑ approaching $\pi/2$, one recovers a symmetric snowflake-plus. The properties of the latter have been studied in great detail in Refs. [3, 5].

For $\pi/2<\vartheta<\pi$, one recovers all these results, but with the second null situated to the left of the vertical axis. [The zone $\vartheta>\pi$ is not allowed by our convention that the confinement region is situated above the horizontal axis, and that the origin is situated on the main separatrix.]

The asymmetric snowflake-minus configuration can be likened to imbalanced double-null divertor, with one null situated near the bottom and the other near the top of

the device. The advantage of the asymmetric snowflake-minus configuration is that the overall expansion of the magnetic field is stronger (due to the proximity to an exact snowflake), and that control over the mutual location of two closely-separated nulls may be simpler than in the case of the nulls separated by a few meters.

V. Finite current density in the divertor region

In the analysis above, we neglected the toroidal plasma current in the divertor region and used condition $\nabla \times \boldsymbol{B}_p = 0$ that lead to Eq. (2). Although the divertor current is typically indeed small [15-18], it is desirable to have some more quantitative measure of its possible effects. For the symmetric snowflake-plus geometry this has been done in Ref. [4]; here we consider a more general asymmetric case. We use the same general approach as in Ref. [4]: we surround the magnetic field null situated on the main separatrix by a circle of a radius small compared to the plasma minor radius a, but sufficiently large to enclose the area of both magnetic field nulls. We assume that the plasma current in the area outside this circle is included in the currents that determine the magnetic field inside the circle; in other words, we assume that their contribution is included in the coefficients l, q, c. In the absence of the current inside the circle, we can use our previous analysis, as then Eq. (2) is applicable in the area of interest. If, however, the toroidal plasma current inside the circle is finite (albeit small), we have to replace the null it in the r.h.s. of Eq. (2) by the term proportional to the current density.

Here we consider the simplest case of a uniform toroidal current density j_d (the subscript "d" stands for the "divertor"). Then, the change of the flux-function (39) would simply consist in the appearance of an additional term

$$\delta\Phi = -\frac{\pi j_d}{c}\left(x^2 + z^2\right), \tag{43}$$

where c (without subscripts) is the speed of light. For our convention that $c_4>0$, the positive sign of j_d corresponds to the divertor current flowing in the same direction as the plasma current. The equation for the flux surfaces becomes

$$\Phi = c_4\left[\left(\frac{3Z}{2}x^2 + 3Xxz - \frac{3}{2}Zz^2 - 3x^2z + z^3\right) - \mu a\left(x^2 + z^2\right)\right] \tag{44}$$

Here, according to Eq. (8),

$$\mu = K\frac{j_d}{\bar{j}}, \tag{45}$$

where $\bar{j}$ is an average over the poloidal cross-section plasma current density and K is a dimensionless coefficient of order unity determined by the details of the current distribution in the bulk plasma. The parameter μ is typically quite small, less than 0.05.

The effect of the divertor currents on the shape of separatrices in the case of the asymmetric snowflake-minus (analogous to that shown in Fig. 5a) is illustrated by Fig. 6. Panel "a" on this figure corresponds to the distance between the nulls approximately equal to $0.05a$ and no current in the divertor (μ=0). On panel "b", we assume that μ=0.05; the general shape of the separatrices does not change significantly compared to the case of no divertor current. More-or-less significant changes appear when μ exceeds 0.075 (panel "c"). At μ>0.09, the structure of the separatrices becomes quite different, with an island of closed flux surfaces formed near the origin. This new configuration is illustrated

by Fig. 7d, where μ=0.1. Similar transformations occur for the snowflake-plus configuration. The corresponding results can be found in Ref. 4 .

VI. Discussion

We derived equations describing the magnetic field of a snowflake divertor in the local approximation, in the vicinity of the second-order null (or the two closely-spaced first-order nulls). Expansion up to the terms of third order in distance is shown to characterize the system with accuracy up to the terms $\sim\varepsilon$, the distance between the nulls divided by the minor radius the minor radius.

Simple algebraic relations have been obtained that relate the coefficients of the power-law representation of the flux function and location of the magnetic field nulls. General characterization of the shape of the separatrix, including its asymptotes, has been presented.

It is shown that the shape of the flux surfaces, aside from trivial transformations related to translations and rotations of the coordinate frame in the poloidal plane, can be characterized by a single parameter. There are four topologically-different configurations possible: an exact snowflake, an exact (symmetric) snowflake-minus, both of which are topologically-unstable, a snowflake-plus, possibly asymmetric, and an asymmetric snowflake-minus. Topological instability of the first two configurations means that the infinitesimal change in the divertor currents leads to their transition to one of the two stable configurations.

The asymmetric snowflake-minus configuration has an interesting property: it allows one to split a strike point on the outer separatrix into two strike points, thereby reducing the heat load by the factor of ~2.

Effects of finite toroidal current density in the vicinity of nulls is analyzed based on a simple model of a uniform current. A conclusion is drawn that the current density has to be quite high in order to change the overall magnetic field structure in the divertor region.

Acknowledgment

This work was performed under the auspices of the U.S. Department of Energy by Lawrence Livermore National Laboratory under Contract DE-AC52-07NA27344.

Appendix

By multiplying Eqs. (16) and (17) (with $B_x=0$, $B_z=0$) by coefficients c_1 and c_4 , adding Eq. (16) to Eq. (17) and subtracting Eq. (16) from Eq. (17), we find an equivalent set of equations for the magnetic field nulls:

$$l_2c_4 - l_1c_1 + 2\left(q_2c_4 + q_3c_1\right)x + 2\left(q_3c_4 - q_2c_1\right)z - 3\left(c_1^2 + c_4^2\right)\left(x^2 - z^2\right) = 0 \qquad \text{(A1)}$$

$$l_2c_1 + l_1c_4 + 2\left(q_2c_1 - q_3c_4\right)x + 2\left(q_3c_1 + q_2c_4\right)z - 6\left(c_1^2 + c_4^2\right)xz = 0 \qquad \text{(A2)}$$

These are two hyperbolas in the x,z plane. By introducing an offset ξ,ζ according to

$$x = x' + \xi, \quad z = z' + \zeta, \qquad \text{(A3)}$$

with

$$\xi = \frac{q_3 c_1 + q_2 c_4}{3\left(c_1^2 + c_4^2\right)}, \quad \zeta = \frac{q_2 c_1 - q_3 c_4}{3\left(c_1^2 + c_4^2\right)}, \tag{A4}$$

one can eliminate linear terms in Eqs. (A1), (A2) and reduce these equations to a canonical form:

$$x'^2 - z'^2 = P, \tag{A5}$$

$$x'z' = Q. \tag{A6}$$

Here

$$P = \frac{l_2 c_4 - l_1 c_1}{3\left(c_1^2 + c_4^2\right)} + \xi^2 - \varsigma^2, \quad Q = \frac{l_2 c_1 + l_1 c_4}{6\left(c_1^2 + c_4^2\right)} + \xi\varsigma. \tag{A7}$$

The set of equations (A5), (A6) has two real solutions,

$$x'_{1,2} = \pm\sqrt{\frac{P}{2} + \sqrt{\frac{P^2}{4} + Q^2}}; \quad z'_{1,2} = \pm(signQ)\sqrt{-\frac{P}{2} + \sqrt{\frac{P^2}{4} + Q^2}}. \tag{A8}$$

Note that the magnetic field nulls in the initial coordinate frame (x,z) are off-set in accordance with Eq. (A3), so that

$$x_{1,2} = x'_{1,2} + \xi; \quad z_{1,2} = z'_{1,2} + \varsigma \tag{A9}$$

In the case where both P and Q are zero, these solutions merge. According to a consideration presented in Ref. 7, this gives rise to an exact snowflake. Unless conditions (11), (12) are satisfied, this snowflake will not be situated in the origin, but rather in the point ($x=\xi$, $z=\zeta$).

References

1. F. Najmabadi and the ARIES team, Fus. Eng. Des., **38**, 3 (1997).

2. M. Kotschenreuther, P.M. Valanju, S.M. Mahajan, J.C. Wiley. Phys. Plasmas, **14**, 072502 (2007).

3. D.D. Ryutov. 'Geometrical Properties of a "Snowflake" Divertor.' Phys. Plasmas, **14**, 064502, June 2007, UCRL-JRNL-227872; D.D. Ryutov. Phys Plasmas, **15**, #6, 2008;

4. D.D. Ryutov. "A snowflake divertor and its properties". Paper D1.002, 34th EPS Conf. on Plasma Phys, Warsaw, July 2-6, 2007 (http://epsppd.epfl.ch/Warsaw/start.htm)

5. D.D. Ryutov, R.H. Cohen, T.D. Rognlien, M.V. Umansky. "Magnetic field structure of a snowflake divertor." "Phys. Plasmas," **15**, 092501 Sept. 2008.

6. D.D. Ryutov, R.H. Bulmer, R.H. Cohen, D.N. Hill, L. Lao, J.E. Menard, T.W. Petrie, L.D. Pearlstein, T.D. Rognlien, P.B. Snyder, V. Soukhanovskii, M.V. Umansky. "A Snowflake Divertor: a Possible Way of Improving the Power Handling in Future Fusion Facilities," Paper IC/P4-8, Proc. 2008 Fusion Energy Conference, IAEA, Vienna, 2009, (http://www-pub.iaea.org/MTCD/Meetings/fec2008pp.asp).

7. M.V. Umansky, R.H. Bulmer, R.H. Cohen, T.D. Rognlien. D.D. Ryutov. "Analysis of geometric variations in high-power tokamak divertors." Nuclear Fusion, **49**, 075005, 2009.

8. D.D. Ryutov, M.V. Umansky. "Ion Drifts in a Snowflake Divertor." "Phys. Plasmas," **17**, 014501, January 2010.

9. F. Piras, S. Coda, I. Furno, J-M. Moret, et al. Plasma Phys. Contr. Fusion, **51**, 055009, 2009.

10. V. Soukhanovskii. "Taming the plasma-material interface with the "snowflake" divertor configuration in NSTX," USBPO News, Issue 42, p. 3, March 15, 2010 (http://burningplasma.org/enews.html)

11. T.W. Petrie, M.R. Wade, N.H. Brooks, M.E. Fenstermacher et al. J. of Nucl. Mat., **363-365**, 416 (2007).

12. M. Kotschenreuther, P. Valanju, S. Mahajan, L.J. Zheng, L.D. Pearlstein, R.H. Bulmer, J. Canik, R. Maingi. Nucl. Fusion, **50**, 035003 (2010).

13. R. Majeski, L. Berzak, T. Gray, et al., Nuclear Fusion, **49**, 055014 (2009).

14. C.S. Pitcher, P.C. Stangeby. PPCF, **39**, 779 (1997).

15. H. Soltwisch. Rev. Sci. Instrum., **57**, 1939 (1986).

16. K. McCormick, F.X. Soldner, D. Eckhartt, et al. Phys. Rev. Lett., **58**,, 491 (1987).

17. ITER Physics Expert Group on Disruption, Plasma Control, and MHD, et al. Nucl. Fusion, **39**, 2577 (1999), see p. 2620.

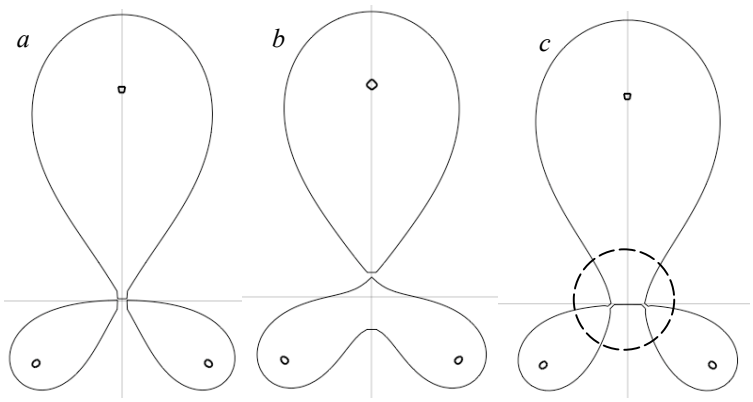

Fig. 1 A 3-wire model of the poloidal field: a) an exact snowflake, b) snowflake-plus; c) snowflake-minus. In this model the configuration is symmetric with respect to a vertical coordinate axis. The present study is concerned with the zone near the origin (a dashed circle in panel c).

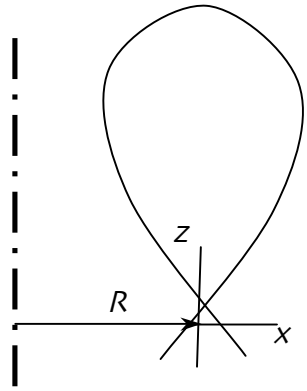

Fig. 2. The coordinate frame. The dashed line represents the tokamak major axis. The origin is deliberately shown as different from the null-point, to emphasize that we assume only that the magnetic field null is situated near the origin, but not necessarily in the origin.

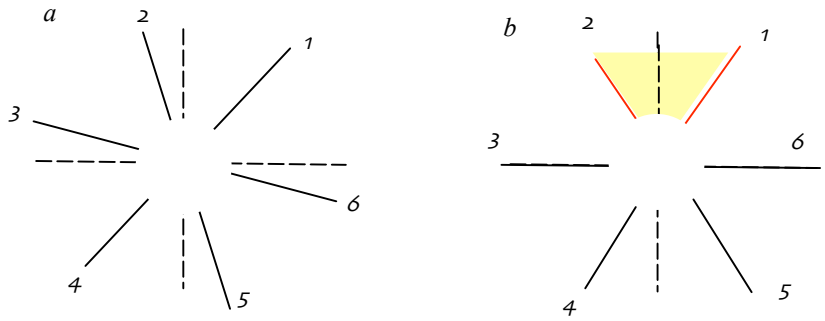

Fig. 3 Asymptotes of the separatrices. Their orientation is independent on the details of the field structure near the origin. To emphasize this fact , the central part is not shown. In Fig b, the frame is turned in such a way, as to put the confinement zone (shaded) into the upper-most segment.

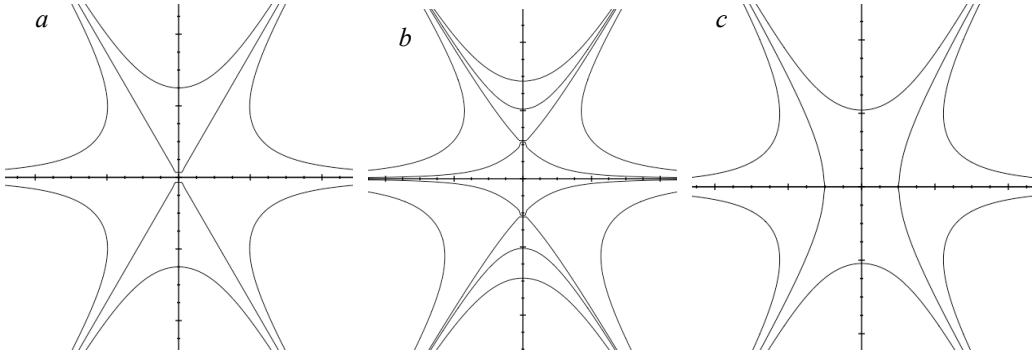

Fig. 4 Snowflake configuration in the symmetric case. For the snowflake-plus case, there is one first order PF null on the main (enclosing the plasma) separatrix. For the snowflake-minus, there are two nulls on the main separatrix.

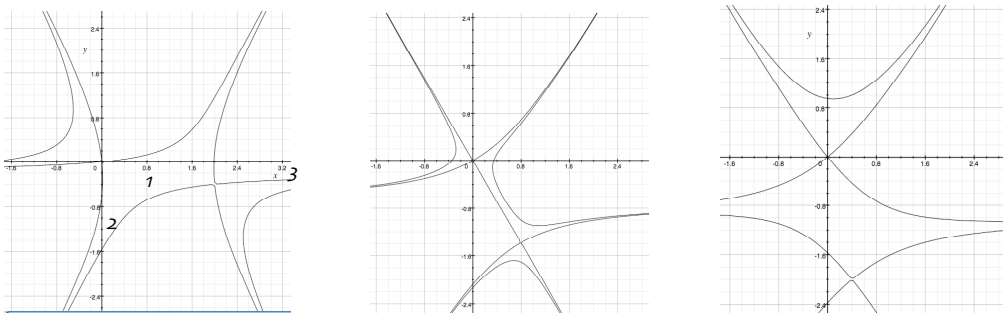

Fig.5 Changes of the magnetic configuration: a) asymmetric snowflake-minus; the second separatrix is adjacent to the main separatrix on the low-field side; see further explanations in the text; b) tilted symmetric snowflake-minus; c) asymmetric snowflake-plus: there is no second separatrix near the main one.

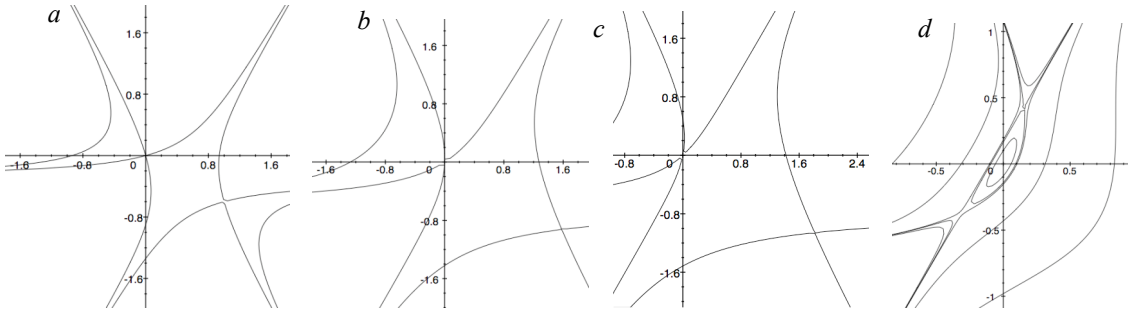

Fig. 6 The effect of the finite current density in the divertor area: a) zero current density (μ=0); b) modest current density (~5% of the current density in the plasma core); c) intermediate current density (7.5%); d) high current density (10%). Note that the scale in panel b is different from that in three other panels (to better illustrate a small area of closed flux surfaces).